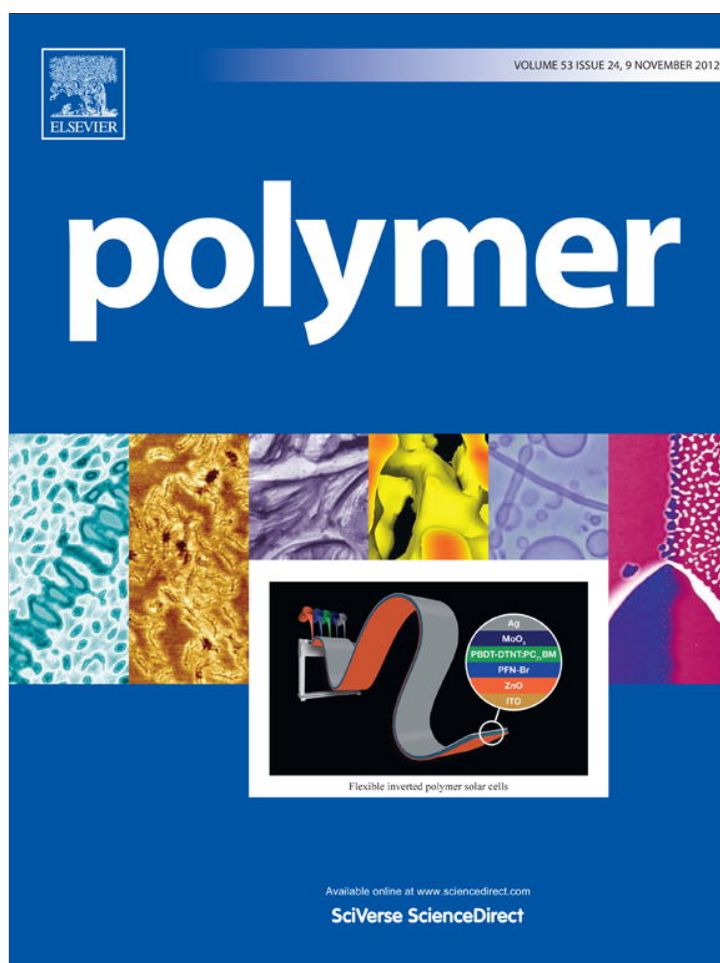


Provided for non-commercial research and education use.
Not for reproduction, distribution or commercial use.

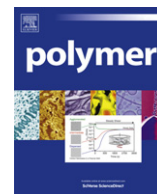


This article appeared in a journal published by Elsevier. The attached copy is furnished to the author for internal non-commercial research and education use, including for instruction at the authors institution and sharing with colleagues.

Other uses, including reproduction and distribution, or selling or licensing copies, or posting to personal, institutional or third party websites are prohibited.

In most cases authors are permitted to post their version of the article (e.g. in Word or Tex form) to their personal website or institutional repository. Authors requiring further information regarding Elsevier's archiving and manuscript policies are encouraged to visit:

<http://www.elsevier.com/copyright>



Structure optimization of self-healing hydrogels formed via hydrophobic interactions

Deniz C. Tuncaboylu^a, Aslihan Argun^b, Melahat Sahin^b, Murat Sari^b, Oguz Okay^{b,*}

^a Bezmialem University, Faculty of Pharmacy, 34093 Istanbul, Turkey

^b Istanbul Technical University, Department of Chemistry, 34469 Maslak, Istanbul, Turkey

ARTICLE INFO

Article history:

Received 17 July 2012

Received in revised form

5 October 2012

Accepted 6 October 2012

Available online 12 October 2012

Keywords:

self-healing

Hydrogels

Hydrophobic associations

ABSTRACT

In an attempt to mimic self-healing functions in biological systems, we investigate here the optimum design parameters of self-healing hydrogels formed by hydrophobic associations in aqueous solutions of wormlike sodium dodecyl sulfate (SDS) micelles. *n*-alkyl (meth)acrylates were used as the hydrophobic comonomer (2 mol %) of acrylamide in the gel preparation. Two structural parameters are crucial for obtaining self-healing gels via hydrophobic interactions. One is the length of the alkyl side chain of the hydrophobe, and the other is the surfactant concentration. In addition, hydrophobic methacrylates generate gels with a higher healing efficiency than the corresponding acrylates due to the limited flexibility of the methacrylate backbones, leading to a greater number of non-associated hydrophobic blocks. These free blocks locating near the fracture surface of the gel samples link each other to self-heal the broken hydrogel. The physical gels without SDS are very tough due to their *sacrificial bonds* that are broken under force and preventing the fracture of the molecular backbone.

© 2012 Elsevier Ltd. All rights reserved.

1. Introduction

Self-healing is a common phenomenon observed in most biological materials such as skin, bones, and wood [1,2]. Autonomous damage repair and resulting healing in such materials often involve an energy dissipation mechanism created by reversible breakable bonds which prevent the fracture of the molecular backbone [3]. In recent years, numerous studies have been conducted to add the self-healing property in synthetic materials [4–11]. The encapsulation approach is based on the introduction of microcapsules containing healing agent within the materials [12]. Release of the healing agent in case of microcrack repairs the materials. The use of reversible chemistry is another approach to obtain self-healing materials [13]. Hydrogen-bonding interactions [14,15], metal-ligand coordination [16], disulfide links [17] have been shown to be useful to create self-healing materials. Deng and co-workers prepared hydrogels with self-healing properties by utilizing reversible acylhydrazone bonds [18]. A complete healing was achieved after a healing time of 24 h while the presence of catalyst decreased the healing time to 8 h.

Recently, we presented a simple strategy to create strong hydrophobic interactions between hydrophilic polymers leading to

the production of self-healing polyacrylamide (PAAm) hydrogels [19,20]. To generate long-lived intermolecular hydrophobic associations making self-healing efficient, blocks of large hydrophobes were incorporated into the hydrophilic PAAm backbone via micellar polymerization technique [21–27]. The key step of our approach is the solubilization of the hydrophobic monomers in a micellar solution of sodium dodecyl sulfate (SDS). As revealed in previous studies [28,29], large hydrophobes such as stearyl methacrylate or docosyl acrylate cannot be solubilized in SDS solutions due to the very low water solubility of the monomers, which restricts the monomer transport through the continuous aqueous phase into the micelles. To overcome this problem, we make use of the characteristics of ionic micelles, namely that the addition of salt such as NaCl into aqueous SDS solutions leads to micellar growth and hence, solubilization of large hydrophobes within the grown wormlike SDS micelles [19]. After solubilization and, after incorporation of the hydrophobic sequences within the hydrophilic polymer chains by micellar polymerization, strong hydrophobic interactions were generated in synthetic hydrogels. The surfactant-containing gels formed using hydrophobic blocks as physical crosslinks exhibit unique characteristics such as insolubility in water but solubility in SDS solutions, non-ergodicity, very large elongation ratios at break, and self-healing [20]. Hydrophobic associations surrounded by surfactant micelles acting as reversible breakable crosslinks are responsible for the extraordinary properties of the hydrogels while the existence of non-associated

* Corresponding author. Tel.: +90 212 2853156; fax: +90 212 2856386.
E-mail address: okay@itu.edu.tr (O. Okay).

hydrophobic blocks is accounted for their high self-healing efficiency (Fig. 1A).

Self-healing gels mentioned above were prepared in 7% SDS solutions and using stearyl methacrylate as the hydrophobic monomer, which is a mixture of 65% n-octadecyl methacrylate and 35% n-hexadecyl methacrylate. Understanding the effects of the hydrophobe size and the surfactant concentration on the self-healing performance of hydrogels could be essential for the optimum design of self-healing soft materials and this was the aim of this study. Here, we used n-alkyl (meth)acrylates of various alkyl chain lengths between 12 and 22 carbon atoms as the physical crosslinker in the gel preparation (Fig. 1B). Dynamic properties of the physical gels were investigated by rheometry, while their large-strain mechanical and self-healing performances were determined by uniaxial elongation or compression tests. To shed light on the role of surfactant micelles in self-healing properties, mechanical properties of the physical gels containing various amounts of SDS were also investigated. It was also of inherent interest to characterize the network chains of self-healing hydrogels to demonstrate their blockiness and associativity. Although the gels were insoluble in water, they could be solubilized in surfactant solutions or, in DMSO at high temperatures, providing structural characterization of the network chains by rheometry, NMR and FTIR techniques. As will be seen below, there are two structural parameters which are crucial for obtaining self-healing gels via hydrophobic interactions. One is the length of alkyl side chain of the hydrophobe, and the other is the surfactant content of the hydrogels.

2. Experimental part

2.1. Materials

Acrylamide (AAM, Merck), sodium dodecyl sulfate (SDS, Merck), ammonium persulfate (APS, Sigma), N,N,N',N'-tetramethylethylenediamine (TEMED, Sigma), and NaCl (Merck) were used as received. Hydrophobic monomers used in this study have linear alkyl side chains 12 to 22 carbons in length (Fig. 1B). They are designated with CxR, where C stands for carbon, x is the number of carbon atoms in side alkyl chain, and R equals to A or M for acrylates and methacrylates, respectively. Commercially available stearyl methacrylate (C17.3M, Aldrich) consisting of 65% n-octadecyl methacrylate and 35% n-hexadecyl methacrylate, was used as received. Since C17.3M is a mixture of two hydrophobes, the average chain length was used in its short name. n-dodecyl methacrylate (C12M, Fluka), n-hexadecyl acrylate (C16A, Tokyo Chemical Industry, TCI), and n-hexadecyl methacrylate (C16M, ABCR) n-octadecyl acrylate (C18A, Fluka), and n-octadecyl methacrylate (C18M, TCI) were used as received. Docosyl acrylate (C22A)

was prepared by the reaction of the 1-docosanol with acryloyl chloride in THF in the presence of triethylamine as a catalyst, as described in the literature [30]. The purity of each batch of C22A was checked by NMR, FTIR, and elemental analysis. Poly(ethylene glycol) of molecular weight 10,000 g/mol (PEG, Fluka) was also used as received.

Micellar copolymerization of AAM with the hydrophobic comonomers was conducted at 25 °C for 24 h in the presence of an APS (3.5 mM) – TEMED (0.25 v/v %) redox initiator system. SDS and NaCl concentrations were set to 7 w/v % (0.24 M) and 0.9 M, respectively. The total monomer concentration and the hydrophobe content of the monomer mixture were also fixed at 10 w/v % and 2 mol %, respectively. Physical gels using C17.3M hydrophobe were also prepared at 5% initial monomer concentration in 0.5 M NaCl solutions containing 7 w/v % SDS. The gel preparation procedure was the same as in our previous studies [19,20]. Shortly, SDS (0.7 g) was dissolved in 9.9 mL NaCl solution at 35 °C to obtain a transparent solution. Then, hydrophobic monomer CxR was dissolved in this SDS–NaCl solution under stirring for 2 h or 4 days (for C22A) at 35 °C. After addition and dissolving AAM for 30 min, TEMED (25 µL) was added into the solution. Finally, 0.1 mL of APS stock solution (0.8 g APS/10 mL distilled water) was added to initiate the reaction. For the mechanical measurements, the copolymerization reactions were carried out in plastic syringes of 4.7 mm internal diameters while, for the rheological measurements, they were conducted within the rheometer.

To obtain hydrogels with various SDS contents, gel samples at the state of preparation were first immersed in water and, after predetermined swelling times, they were dialyzed using Snake Skin membranes (3500 MWCO, Pierce, Thermo Scientific, Rockford, IL) for 4 days against 0.5 M NaCl solution containing required amounts of SDS and 5 to 7 w/v % PEG, that was changed every other day. By the osmotic stress adjusted with the PEG concentration in the external solution, water molecules inside the hydrogels moved into the outer solution through the dialysis membrane so that a series of gels of the same polymer concentration (10 w/v %) but with various amounts of SDS between 0 and 7% were obtained.

2.2. Solubilization tests of the hydrophobes in SDS–NaCl solutions

The amount of the hydrophobic monomers solubilized in SDS micelles was estimated by measuring the transmittance of SDS–NaCl solutions at 35 °C containing various amounts of hydrophobes on a T80 UV–visible spectrophotometer. The transmittance at 500 nm was plotted as a function of the added amount of the hydrophobe in the SDS–NaCl solution and, the solubilization extent was determined by the curve break (Fig. S1).

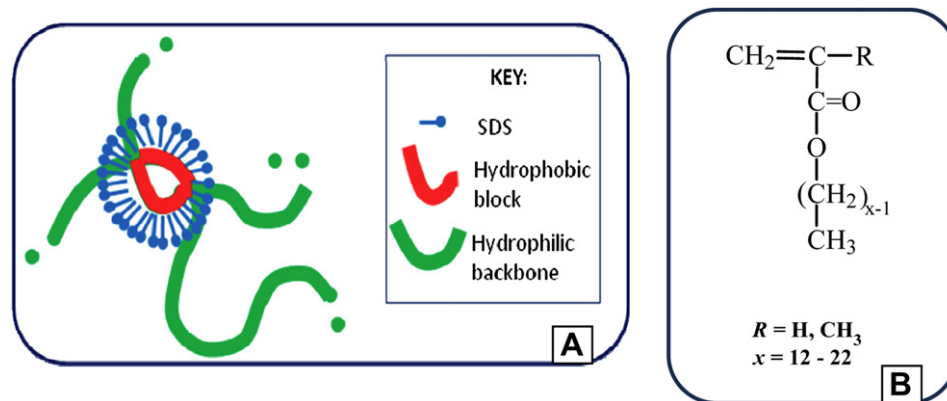


Fig. 1. A) Cartoon showing the physical crosslink of self-healing gel and B) structure of the hydrophobic monomers used as physical crosslinkers.

2.3. Rheological experiments

Gelation reactions were carried out at 25 °C within the rheometer (Gemini 150 Rheometer system, Bohlin Instruments) equipped with a cone-and-plate geometry with a cone angle of 4° and diameter of 40 mm. The instrument was equipped with a Peltier device for temperature control. The reactions were monitored at an angular frequency ω of 6.3 rad/s and a deformation amplitude $\gamma_o = 0.01$. After a reaction time of 3 h, the dynamic moduli of the reaction solutions approached limiting values (Fig. S2). Then, frequency-sweep tests at $\gamma_o = 0.01$ were carried out over the frequency range 0.063–250 rad/s.

2.4. Mechanical tests

The measurements were performed in a thermostated room at 25 ± 0.5 °C on a Zwick Roell test machine using a 10 N load cell. Cyclic compression experiments were performed on cylindrical hydrogel samples of 4.7 mm diameter and 6 mm length placed between the plates of the instrument. Before the test, an initial compressive contact to 0.004 ± 0.003 N was applied to ensure a complete contact between the gel and the plates. Cyclic tests were conducted with a compression step performed at a constant crosshead speed of 5 mm/min to a maximum load (varied between 0.5 and 5 N), followed by immediate retraction to zero displacement and a waiting time of 2 min, until the next cycle of compression. Load and displacement data were collected during the experiment. Compressive stress was presented by its nominal σ_{nom} or true values $\sigma_{true} (= \lambda \sigma_{nom})$, which are the forces per cross-sectional area of the undeformed and deformed gel specimen, respectively, while the strain is given by λ , the deformation ratio (deformed length/initial length).

Uniaxial elongation measurements were performed on cylindrical hydrogel samples of 4.7 mm in diameter under the following conditions: Crosshead speed = 50 mm/min, sample length between jaws = 13 ± 3 mm. Samples were held on the test machine between clamps altered with anti-slip tape (Tesa, 25 × 15 mm) together with cyano acrylate adhesive (Evobond) or, with wood strips to better grip the slippery gel samples. The ultimate strength, percentage elongation at break, and toughness were recorded. Tensile modulus was calculated from the slope of stress-strain curves between elongations of 5% and 15%. Cyclic elongation tests were conducted at a constant crosshead speed of 50 mm/min to a maximum elongation ratio (varied between 100 and 400%), followed by retraction to zero force and a waiting time of 7 min, until the next cycle of elongation. For reproducibility, at least six samples were measured for each gel and the results were averaged.

2.5. Solubilization of gels and characterization of network chains

Hydrogel samples were immersed in a large excess of water at 24 °C for at least 30 days by replacing water every second or third day, until the SDS concentration in the external solution decreases below the detection limit of the methylene blue method (0.20 mg L^{-1}) [31]. Then, the equilibrium swollen gel samples were taken out of water and freeze dried. The measurements of the gel fraction W_g (mass of dry, extracted network/mass of the monomers in the comonomer feed) revealed that W_g equals 1.0 for all the physical gels indicating existence of strong hydrophobic associations. For spectroscopic characterization, FTIR spectra of dry, extracted networks were recorded on a Perkin–Elmer FTIR Spectrum One-B spectrometer.

Although the physical gels were insoluble in water, they could be solubilized in DMSO at 80 °C. ^1H NMR spectra of the disintegrated gels were recorded on a Bruker 250 MHz spectrometer

using ca. 10 mg polymer network samples dissolved in 1 mL of d_6 -DMSO at 80 °C. The physical gels could also be dissolved in aqueous SDS or SDS-NaCl solutions. Even solubility tests conducted in a limiting volume of water at a high temperature provided complete solubilization of gels due to the surfactant molecules moving from the gel to the solution phase. For characterization purposes, solubilization of gels was carried out according to the following procedure. Gel sample was immersed into 10 mL of 0.5 M NaCl solution for a duration of 3 days at 50 °C until complete solubilization. To fix the concentration of both the dissolved network chains and SDS in the solution, the mass of the gel sample was changed depending on the initial monomer concentration at the gel preparation and, appropriate amount of SDS was added. In this way, homogeneous 0.5 M NaCl solutions containing 0.5 w/v % polymer and 0.7 w/v % SDS were obtained. For comparison, PAAm solutions were prepared as described above, except that the micellar polymerization was carried out in the absence of the hydrophobe. The solutions were then subjected to frequency-sweep tests at $\gamma_o = 0.01$ and viscosity measurements at various shear rates between 10^{-2} and 10^3 s^{-1} .

3. Results and discussion

3.1. Effect of hydrophobe

Physical gels were prepared by the micellar copolymerization of AAm with 7 different n-alkyl (meth)acrylates (*hydrophobes*) having linear alkyl side chains 12 to 22 carbons in length. Hydrophobe content of the monomer mixture and the total monomer concentration were fixed at 2 mol % and 10%, respectively. As revealed in previous studies [19], copolymerization conducted in 7 w/v % SDS solution but in the absence of NaCl led to the formation of a polymer solution with an elastic modulus of a few Pascal's and a loss factor larger than unity. Upon addition of NaCl into the reaction solution, however, the elastic modulus rapidly increased demonstrating solubilization of the hydrophobes in the micellar solution and incorporation of the hydrophobic sequences into the polyacrylamide (PAAm) chains to form intermolecular hydrophobic associations. To determine the amount of NaCl required for complete solubilization of the hydrophobes in the micellar solution, solubility tests were conducted using the most hydrophobic monomer C22A, together with C17.3M and C18A. Fig. 2A shows the hydrophobe solubility in 7 w/v % SDS solution as a function of the added amount of NaCl. The solubility increases with increasing salt concentration due to the simultaneous increase of the micellar size [19]. Among these hydrophobes, enhancement of the solubility is largest for C18A, followed by C17.3M and C22A. Although the average alkyl side chain of C17.3M is shorter than that of C18A, the methacrylate group of the former molecule seems to be responsible for its less solubility in the micellar solution. Solubility results also revealed that the complete solubilization of C22A in the micellar copolymerization system requires a salt concentration of 0.9 M NaCl, which was fixed for all the gelation reactions.

Copolymerizations of AAm with 2 mol % of the hydrophobes in SDS-NaCl solution were first monitored within the rheometer at a strain amplitude of 1% and at an angular frequency of 6.3 rad/s. During the reactions, both the elastic G' and viscous moduli G'' increased while the loss factor $\tan \delta (=G''/G')$ decreased rapidly and then approached plateau values after 1–2 h (Fig. S2). Plateau values of $\tan \delta$ were between 0.2 and 0.4 for all hydrophobes indicating formation of viscoelastic gels. Fig. 2B shows the frequency dependences of G' (filled symbols) and G'' (open symbols) of the physical gels formed using C18A, C17.3M, and C22A. All the gel samples exhibit time-dependent dynamic moduli with a plateau elastic modulus at high frequencies ($>10^2 \text{ rad/s}$), demonstrating the

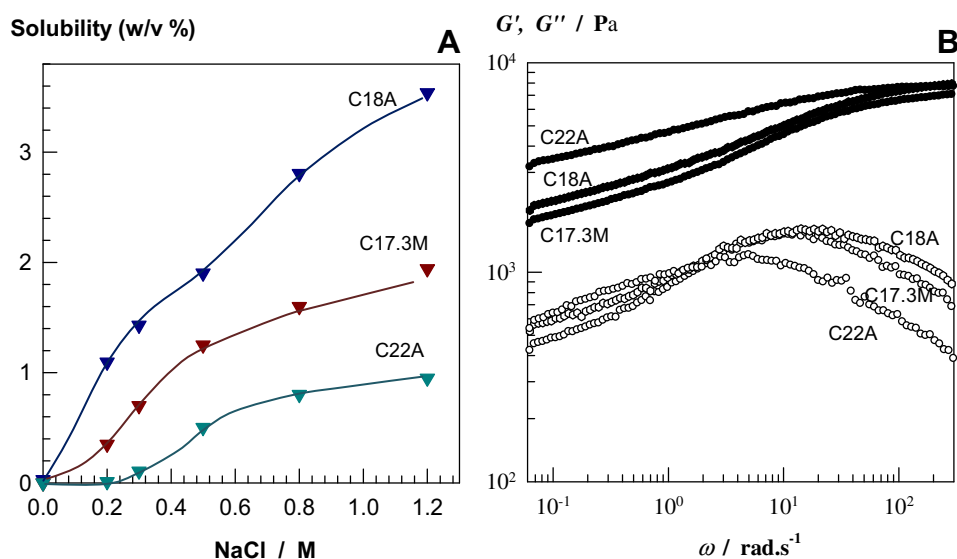


Fig. 2. A) Solubility of the hydrophobic monomers C17.3M, C18A, and C22A in SDS - NaCl solutions at 35 °C plotted against NaCl concentration. SDS = 7 w/v %. B) G' (filled symbols) and G'' (open symbols) of the physical gels shown as a function of angular frequency ω measured after 3 h of reaction time. $\gamma_0 = 0.01$. Type of the hydrophobe indicated.

temporary nature of the hydrophobic associations having lifetimes of the order of seconds to milliseconds. The physical gel formed using C22A exhibits a much slower relaxation at low frequencies compared to other hydrophobes (Fig. 2B and Fig. S3), as expected given that the activation energy for disengagement of hydrophobic blocks increases with hydrophobe length [32–34]. Close inspection of the frequency-sweep data of gels also shows that (i) at a fixed length of the alkyl side chain, hydrophobic methacrylates produce gels with a higher loss factor $\tan \delta$ as compared to the acrylates, indicating dissipation of a greater amount of energy, and (ii) $\tan \delta$ decreases as the size of the hydrophobe increases indicating increasing elasticity of the physical gels (Fig. S4).

To highlight the effect of hydrophobe size on the mechanical properties and self-healing performance of gels, cylindrical gel samples after a reaction time of 24 h were subjected to uniaxial elongation and compression tests. Fig. 3A represents stress-strain data of the physical gels, as the dependence of the nominal stress σ_{nom} on the deformation ratio λ . In compression tests ($\lambda < 1$), although no break was detected in $\sigma_{\text{nom}} - \lambda$ plots, $\sigma_{\text{true}} - \lambda$ plots given in Fig. S5 illustrate that λ at failure is around 0.04 indicating that all gels are stable up to a compression ratio of 96%. In elongation tests, λ at break is larger than 16, i.e., the elongation exceeds 1500% for all the physical gels while the ultimate strength of gels formed using hydrophobic acrylates is larger (30–65 kPa) than those formed using methacrylates (20–30 kPa).

The large strain properties of the physical gels were compared by cyclic compression tests conducted up to a strain below the failure. The tests were conducted by compression of cylindrical gel samples at a constant crosshead speed to a predetermined maximum load, followed by immediate retraction to zero displacement. After a waiting time of 2 min, the cycles were repeated twice. In all cases, the loading curve of the compressive cycle was different from the unloading curve indicating damage in the gel samples and dissipation of energy during the cycle. In Fig. 3B, typical successive loading–unloading cycles of the gel samples formed using C17.3M, C18A, and C22A are shown as the dependence of the nominal stress σ_{nom} on the deformation ratio λ . It is seen that the behavior of the virgin samples can be recovered after a waiting time of 2 min without stress. The reversibility of loading/unloading cycles was observed in all gels

(Fig. S6). The perfect superposition of the successive loading curves demonstrates that the damage done to the gel samples during the loading cycle is recoverable in nature. This behavior is similar to that of the hydrogels formed by dynamic crosslinkers [35,36]. The energy U_{hys} dissipated during the compression cycle was calculated from the area between the loading and unloading curves (Fig. S6). For gels formed using 7 different hydrophobes, the hysteresis energies U_{hys} were 5 ± 1 , 8 ± 2 , and 14 ± 2 kJ/m³ for a maximum load of 1, 2, and 4 N, respectively. Since the loading/unloading cycles are reversible, U_{hys} is associated with the number of reversible broken hydrophobic associations [35,37,38]. Thus, this number increases with increasing maximum load, i.e., with increasing maximum strain during the loading step. The reversible disengagements of the hydrophobic units from the associations under an external force also point out the self-healing properties of the physical gels.

To quantify the self-healing efficiency, tensile testing experiments were performed using cylindrical gel samples of 4.7 mm in diameter and 6 cm in length. Gel samples were cut in the middle and then, the two halves were merged together within a plastic syringe (of the same diameter as the gel sample) at 25 °C by slightly pressing the piston plunger. The healing time was set to 30 min and each experiment was carried out starting from a virgin sample. In Fig. 4A, the elongation ratios at break of the virgin ($\lambda_{b,0}$) and healed gel samples (λ_b) are plotted against the type of the hydrophobe used in the gel preparation. The healing efficiencies ϵ_H of gels calculated as $\epsilon_H = (\lambda_b/\lambda_{b,0})10^2$ are shown in Fig. 4B. λ_b approaches to $\lambda_{b,0}$, that is, the efficiency ϵ_H increases with increasing length of the alkyl side chain and, the highest value of the healing efficiency was observed in the physical gel formed using C18M hydrophobe. The efficiency ϵ_H decreases again as the alkyl chain length of the hydrophobe is further increased. This reveals that the ability of the gels to self-heal depends critically on the length of side alkyl chains. Hydrophobes having an alkyl side chain 18 carbons in length generate strongest self-healing in the physical gels.

Another important result of Fig. 4B is that the hydrophobic methacrylates generate physical gels with a higher healing efficiency than the corresponding acrylates. For instance, at an alkyl chain length of 18 carbon atoms, the healing efficiency increases from 34% to 88%, by replacing acrylate (C18A) with methacrylate

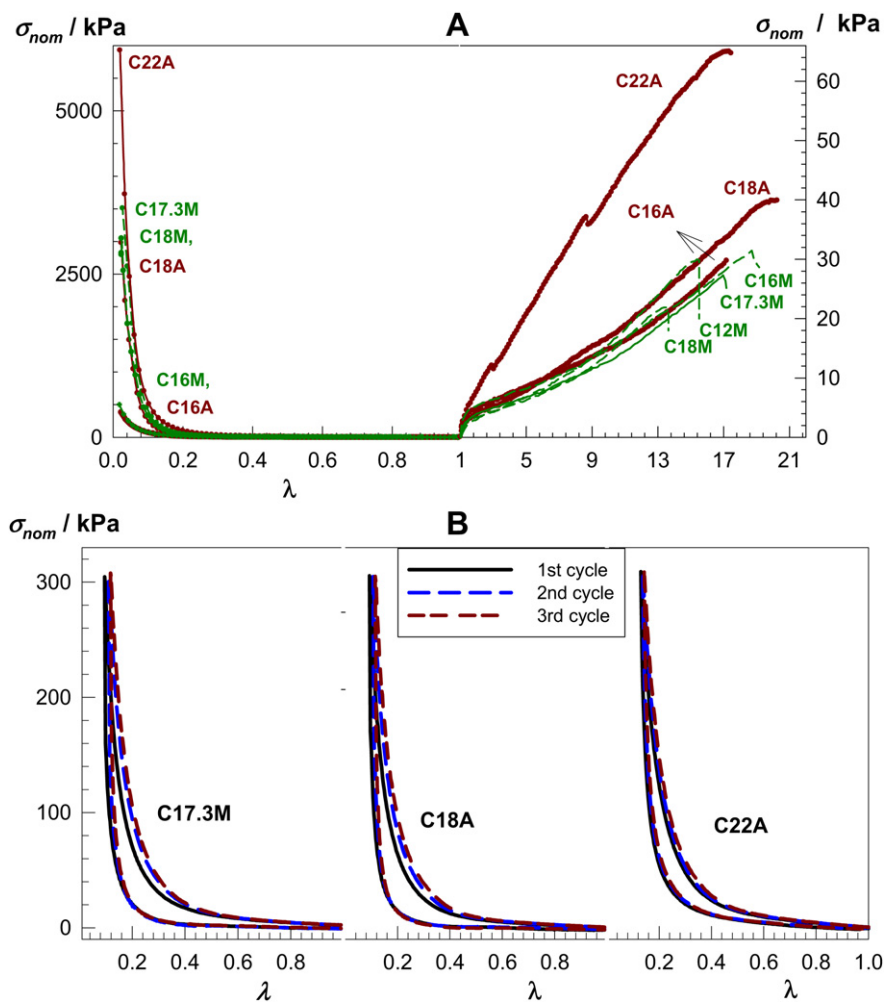


Fig. 3. A) Stress-strain curves of the physical gels under compression and elongation as the dependence of nominal stress σ_{nom} on the deformation ratio λ . The type of the hydrophobes indicated. B) Three successive loading/unloading cycles are shown for gel samples formed using C17.3M, C18A, and C22A. Maximum load = 5 N.

(C18M). A similar trend is seen when comparing the gels formed by C16A and C16M hydrophobes (29% versus 49%). This significant effect of the backbone methyl group on self-healing is attributed to the limited flexibility of the methacrylate backbones. Previous

works on side chain crystalline polymers show that both the melting temperature and the degree of crystallinity of polymers formed by methacrylates are lower than those formed by acrylates [39], indicating that the methacrylate backbone hinders the

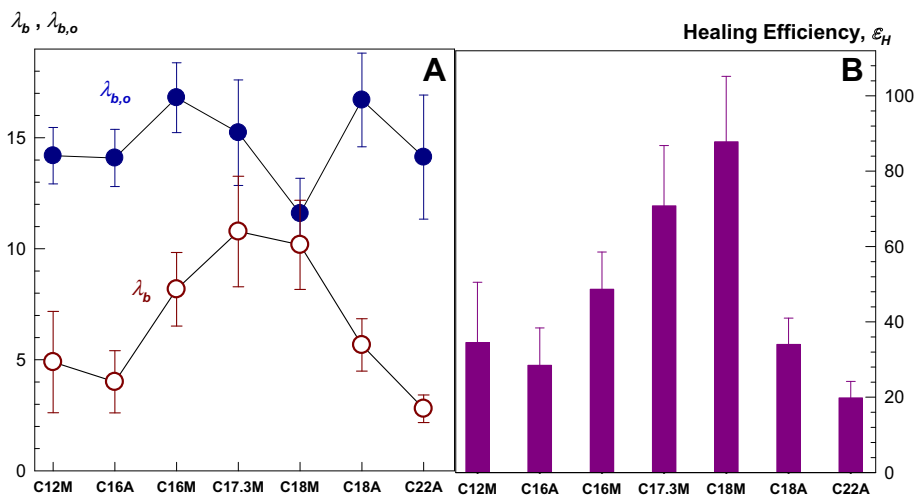


Fig. 4. A) Elongation ratio at break of healed λ_b and virgin gel samples $\lambda_{b,0}$ and B) the healing efficiency ϵ_H for the gels formed using 7 different hydrophobes.

alignment of side alkyl chains. Thus, one may expect that, due to the limited flexibility of methacrylate backbone, the number of associations formed by hydrophobic methacrylates is reduced so that a larger fraction of non-associated hydrophobic blocks exists in the gel samples. This is also supported by the lower ultimate strength and higher loss factor of gels formed using hydrophobic methacrylates (Fig. 3A and Fig. S4). As the free hydrophobic blocks locating near the fracture surface of the gel samples link each other to self-heal the broken hydrogel, the higher the number of free hydrophobic blocks, the higher is the healing efficiency. As a consequence, increasing number of non-associated blocks in gels formed by methacrylates leads to higher self-healing efficiencies compared to acrylates.

3.2. Effect of surfactant

Another critical parameter for the self-healing performance is the concentration of surfactant micelles in gels. In the previous section, the physical gels were characterized at their preparation states, i.e., in the presence of 7 w/v % SDS. However, the gels where SDS had been removed after their preparation exhibited very different behavior. For instance, Fig. 5A and B show the frequency dependencies of G' (filled symbols), G'' (open symbols), and $\tan \delta$ (lines) for the gels formed using C17.3M, C18A, and C22A hydrophobes with (A) and without SDS (B). It is seen that, after extraction of SDS, the dynamic moduli of the physical gels become time independent and $\tan \delta$ decreases from above to below 0.1 indicating increasing lifetime of the hydrophobic associations. Similar results were also obtained for gel samples formed using other hydrophobic monomers (Fig. S7). The marked change in the internal dynamics of gels is attributed to the strengthening of the hydrophobic associations in the absence of surfactant micelles [20],

so that their dynamic behavior approaches to that of the chemically crosslinked hydrogels.

The effect of surfactant on the mechanical properties of the physical gels was investigated by conducting mechanical tests on gel samples with varying SDS content. The gels formed using C17.3M hydrophobe were chosen for this set of experiments. For the micellar polymerization reactions, a salt concentration of 0.5 M NaCl was sufficed to solubilize C17.3M completely in 7% SDS solution (Fig. 2A). After preparation of the physical gels in 0.5 M NaCl solution containing 7% SDS, they were dialyzed against SDS-NaCl-PEG solutions, as detailed in the experimental part, to obtain gel samples having the same polymer concentration (10 w/v %) but varying SDS contents between 0 and 7 w/v %. Tensile modulus, ultimate strength, elongation at break, and toughness data for gels with different SDS % are summarized in Fig. 6. An enhancement in the mechanical strength of the gel is seen when its SDS content is decreased and, this enhancement becomes dramatic between 1 and 0% SDS. Gels without SDS exhibit high modulus (~ 50 kPa), high ultimate strength (~ 200 kPa) and toughness (~ 1 MJ/m³) due to the increasing lifetime of hydrophobic associations in the absence of SDS (Fig. 5). Elongations at break exhibit a slight dependence on the SDS content and decreases from 1600 to 800 % with decreasing amount of SDS. Thus, the mechanical properties of the physical gels can be varied greatly by changing SDS %.

In the tensile testing described above, it was observed that the self-healing ability of gels gradually disappears as the SDS content is decreased. However, the self-healing efficiency cannot be quantified as in the previous section due to the fact that the gel samples were too slippery because of the dialysis procedure applied to adjust their SDS contents. Tests conducted by firmly stretching virgin and healed gel samples by hand showed that the gels lost their capacity to self-heal at or below 3% SDS content. Cyclic tensile tests also confirmed the lack of a self-healing mechanism in gel samples containing no SDS. Fig. 7A and B show the results of 3 successive cyclic tensile tests conducted on gels with and without SDS, respectively. The tests were carried out up to a maximum strain (λ_{\max}) of 5 with a waiting time of 7 min between cycles. The gel sample with SDS exhibits reversible loading/unloading cycles indicating that the original network structure can be recovered when the damaged gel sample is left to rest for 7 min without stress. Visual observation indeed showed that the residual elongation after the first cycle (denoted by an asterisk in Fig. 7A) decreased with increasing waiting time and disappeared after 7 min, so that the next loading cycle follows the path of the first loading. Thus, similar to the cyclic compression tests (Fig. 3B), cyclic tensile tests also confirm the existence of reversible breakable crosslinks in SDS containing gels.

In contrast, the gel sample without SDS exhibits very different behavior (Fig. 7B). Although the loading curve of the first cycle is different from the unloading and a significant hysteresis occurs as in the case of SDS containing gel, the second and the third cycles are almost elastic with a small amount of hysteresis and, they closely follow the path of the first unloading. This clearly indicates the occurrence of an irrecoverable damage to the gel sample during the first cycle, leading to a permanent residual elongation. Fig. 8A shows the results of 8 successive loading/unloading cycles with increasing maximum strain λ_{\max} from 2 up to 9 (100–800% elongations), with 7 min waiting time between each cycle. For clarity, successive cycles are shown by the solid and dashed curves. An idealized view of two successive cycles is also shown in Fig. 8B. It is seen that each loading curve with $\lambda_{\max} > 3$ consists of two regions.

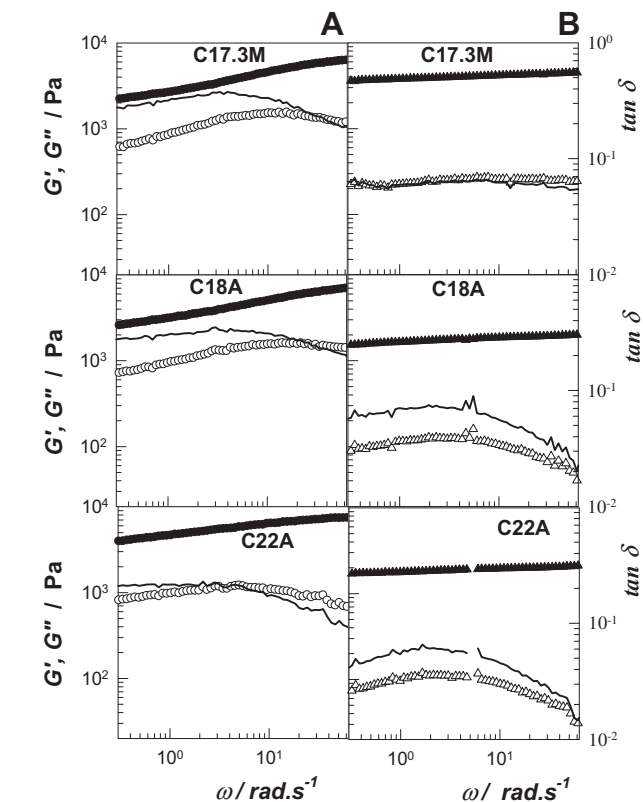


Fig. 5. G' (filled symbols), G'' (open symbols) and $\tan \delta$ (lines) of gels with (A) and without SDS (B) shown as a function of angular frequency ω . $\gamma_0 = 0.01$. The type of the hydrophobes indicated.

- 1) Elastic region that closely follows the path of the unloading curve of the previous cycle,

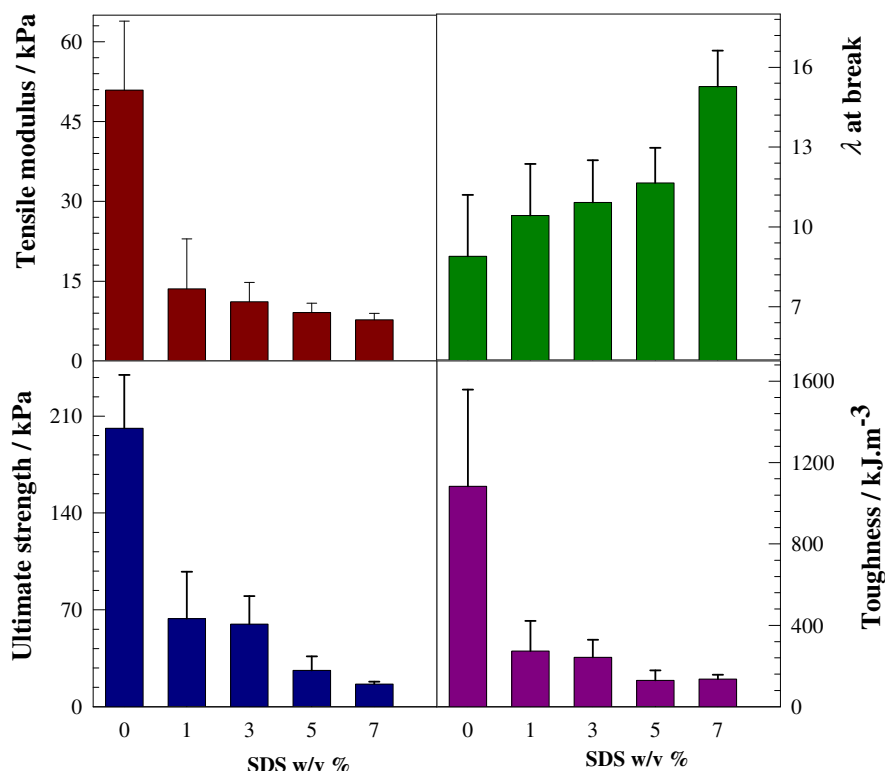


Fig. 6. Tensile modulus, elongation ratio λ at break, ultimate strength, and toughness of gels formed using C17.3M hydrophobe shown as a function of SDS %.

2) Damage region continuing the loading curve of the previous cycle.

The transition from elastic to damage region occurs at the maximum strain λ_{\max} of the previous cycle. For example, the loading curve of cycle-5 ($\lambda_{\max} = 5$) follows the unloading and loading curves of cycle-4 between $\lambda = 1-4$ and $\lambda = 4-5$, respectively. Thus, due to the irreversible damage done during the previous cycle, additional damage only occurs at a higher maximum strain. The dotted red curve in Fig. 8A shows the cycle conducted on a virgin gel sample up to $\lambda_{\max} = 5$. Since there is no previous damage to the gel sample, the loading curve follows the second region of the loading curves of cycles with $\lambda_{\max} \leq 5$. Thus, the hysteresis of the first cycle is related to irreversible fracture of a part of the hydrophobic associations whose extent increases with increasing λ_{\max} , i.e., with increasing maximum strain during the loading step. The results also verify the loss of self-healing ability in

gel samples containing no SDS. We note that the behavior of the present gels without SDS shown in Fig. 7B and Fig. 8A is very similar to that of double-network (DN) hydrogels [37,40], where the first-cycle hysteresis occurs due to the irreversible fracture of covalent bonds in the highly crosslinked primary network.

We should emphasize that, although the physical gels without SDS have no self-healing ability, they are very tough with toughness values about one order of magnitude higher than those of SDS containing gels (Fig. 6). This behavior of gels containing no SDS is also completely different from that of chemically crosslinked gels, which are brittle due to their very low resistance to crack propagation. We hypothesize that the enhancement in the mechanical strength of the physical gels without SDS arises from the *sacrificial bonds* broken during the first cycle [41]. Many natural materials have such sacrificial bonds, which are defined as the bonds that break before the molecular backbone is broken [3]. These bonds are weaker than the covalent bonds of molecular backbones and

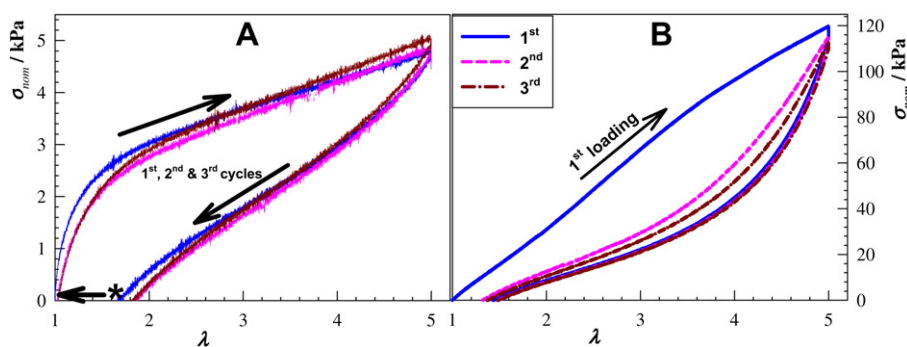


Fig. 7. Three successive loading/unloading cycles of gels with 7% SDS (A) and without SDS (B). $\lambda_{\max} = 5$. Hydrophobe = C17.3M. Waiting time between cycles = 7 min. Crosshead speed = 50 mm/min.

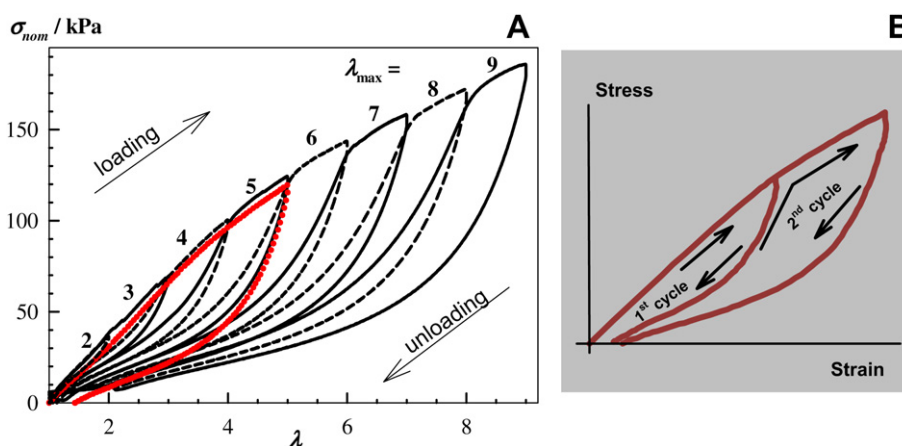


Fig. 8. (A): 8 Successive loading/unloading cycles for different values of λ_{\max} indicated. The dotted red curve represents the cycle conducted on a virgin gel sample ($\lambda_{\max} = 5$). The tests were carried out using gel samples without SDS. (B): Cartoon representing an idealized view of two successive cycles. (For interpretation of the references to color in this figure legend, the reader is referred to the web version of this article.)

greatly increase the toughness of biomaterials by creating an energy dissipation mechanism under external force [42]. For the present system, the energy dissipation mechanism created by the hydrophobic associations that are destroyed under the applied force prevents the fracture of the molecular backbone up to an elongation ratio of about 800%.

3.3. Characterization of the network chains of self-healing gels

Previous sections demonstrate extraordinary mechanical performance of the physical gels formed by hydrophobic associations. To obtain more information about the incorporation behavior of the hydrophobes, solubilization tests were carried out by immersing the physical gels in several solvents and solutions. Although the gels were insoluble in water due to the strong hydrophobic interactions, they could be dissolved in SDS solutions as well as in DMSO at 80 °C, providing microstructural characterization of the network chains. Physical gels formed using 2 mol % C17.3M hydrophobe were chosen for characterization. The initial monomer concentration C_0 was again 10 w/v %. To demonstrate the blockiness of the network chains, the gels were also prepared at $C_0 = 5$ w/v %. Since the aggregation number of SDS micelles in 0.5 M NaCl solution is 200 [19], assuming a homogeneous distribution of the hydrophobe along the micelles, the length N_H of the

hydrophobic blocks in the network chains will be 12 and 23 for gels formed at $C_0 = 5$ and 10%, respectively. In the following, the network chains isolated from the physical gels with $N_H = 12$ and 23 are denoted by P1 and P2, respectively.

Fig. 9 shows FTIR spectra of the network chains together with PAAm for comparison. Both P1 and P2 exhibit the characteristic bands at 2920 cm^{-1} and 2850 cm^{-1} due to the stretching of the methylene groups of C17.3M units, which are absent in PAAm chains (dashed curve). ^1H NMR spectra of the same polymers in d_6 -DMSO also shown in Fig. 9 exhibit characteristic protons emerging from C17.3M units. Peak A at 0.9 ppm arises due to the protons of α -methyl backbone and of the terminal methyl of the alkyl chain, while the peak B at 1.2 ppm was caused by the protons attached to carbon atoms on the side alkyl chain of C17.3M units. Although NMR technique was not sensitive enough for the determination of copolymer microstructure due to the low hydrophobe content, increasing peak intensities with increasing N_H indicates blockiness of the polymers.

In parallel with this observation, viscometric and rheological behavior of the network chains in 0.7% SDS solutions also showed a substantial increase in the associativity with increasing N_H , i.e., with increasing length of the hydrophobic blocks. Fig. 10A shows shear rate dependence of the viscosity of 0.5 w/v % solutions for the polymers P1 and P2 together with the PAAm homopolymer. A

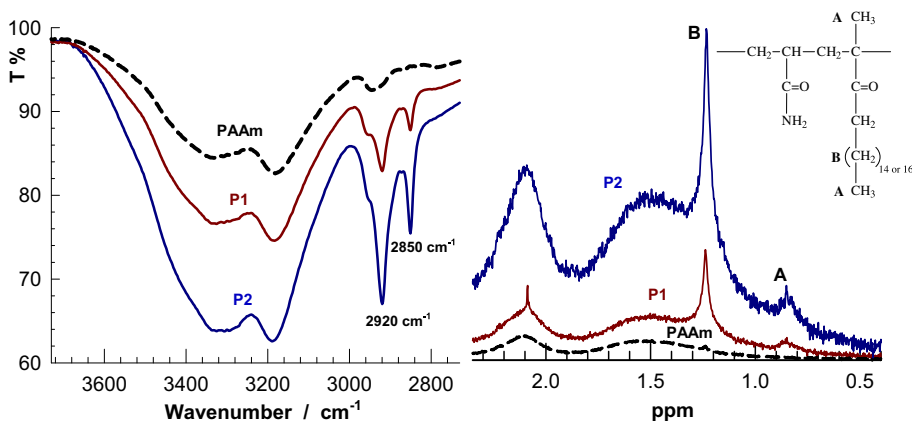


Fig. 9. FTIR and ^1H NMR spectra of the network chains together with the spectra of PAAm. P1 and P2 denote the polymers formed at 5 and 10% initial monomer concentrations, respectively.

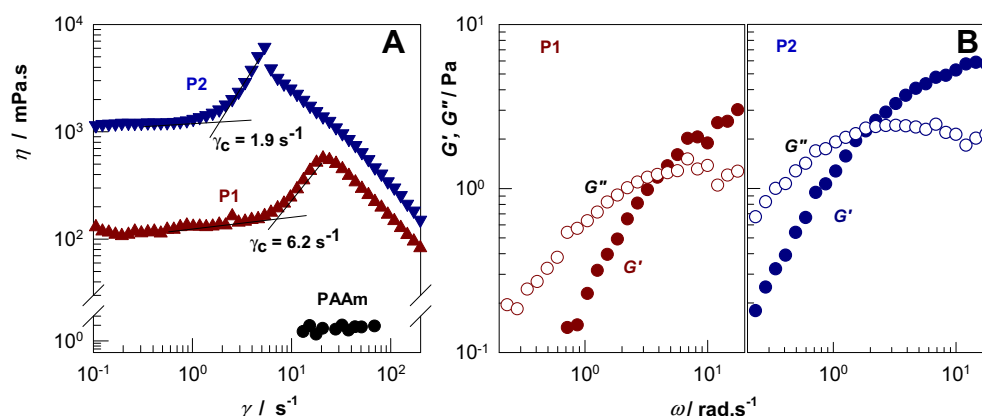


Fig. 10. The viscosity η /shear rate curves (A) and frequency-sweeps (B) for the solutions of P1, P2 and PAAm. Polymer = 0.5 w/v %. SDS = 0.7 w/v %. NaCl = 0.5 M. Temperature = 35 °C.

strong enhancement of the viscosities of both P1 and P2 solutions as compared to PAAm solution demonstrates the existence of hydrophobic blocks in the network chains. The solutions of the network chains exhibit a Newtonian plateau at low shear rates followed by an abrupt shear thickening region before the onset of shear thinning. The shear thickening region is typical for associative flexible polymers and, is a result of the formation of transient intermolecular hydrophobic associations [43–45]. These associations are favorable at a certain degree of coil deformation while they become disrupted at higher shear rates. The critical shear rate γ_c for the onset of shear thickening behavior yields a characteristic time $\tau_c = 1/\gamma_c$ that scales with zero-shear viscosity, which is verified by the data in the figure. For P1 and P2 solutions, τ_c times are 0.53 and 0.16 s with zero-shear viscosities of 1.18 and 0.11 Pa s, respectively. Thus, despite the same hydrophobe level, solutions of P2 (network chains of self-healing gels) exhibit smaller τ_c values and higher viscosities compared to P1 solutions demonstrating increasing associativity of the polymers due to the increasing length of the hydrophobic blocks. The results are also confirmed by the frequency-sweep tests, as shown in Fig. 10B. The characteristic relaxation times τ_R , as determined by the crossover frequency ω_c at which G' and G'' values are equal ($\tau_R = \omega_c^{-1}$) are 0.31 and 0.53 s for P1 and P2 solutions, respectively. This also indicates strong associativity of the network chains of self-healing hydrogels investigated in this study.

4. Conclusions

Two structural parameters are crucial for obtaining self-healing gels via hydrophobic interactions. One is the length of the alkyl side chain of the hydrophobe, and the other is the surfactant concentration in gels. Hydrophobes with an alkyl chain length of 18 carbon atoms generate strongest self-healing in the physical gels. In addition, hydrophobic methacrylates such as n-octadecyl methacrylate (C18M) produce gels with a higher healing efficiency than the corresponding acrylates. The significant effect of the backbone methyl on self-healing is due to the limited flexibility of the methacrylate backbones leading to a greater number of non-associated hydrophobic blocks. These non-associated hydrophobic blocks locating near the fracture surface of the gel samples link each other to self-heal the broken hydrogel.

Another important question addressed in this study was how the surfactant concentration affects the mechanical properties of the hydrogels. It was shown that the mechanical properties of the physical gels can be varied greatly by changing their SDS contents.

Due to the strengthening of the hydrophobic associations in the absence of surfactant micelles, decreasing SDS content leads to a marked increase in the mechanical strength of gels while, simultaneously, the ability of the gels to self-heal disappears. Although the physical gels without SDS exhibit no self-healing ability, they are very tough indicating an energy dissipation mechanism. By cyclic tensile tests, we demonstrated that the enhancement in the mechanical strength of the physical gels without SDS arises from the *sacrificial bonds* that are broken under the applied force and thus preventing the fracture of the molecular backbone up to high elongation ratios.

Acknowledgment

Work was supported by the Scientific and Technical Research Council of Turkey (TUBITAK) and International Bureau of the Federal Ministry of Education and Research of Germany (BMBF), TBAG –109T646. O. O. thanks Turkish Academy of Sciences (TUBA) for the partial support.

Appendix A. Supplementary data

Supplementary data related to this article can be found at <http://dx.doi.org/10.1016/j.polymer.2012.10.015>.

References

- [1] Fratzl PJR. Soc Interface 2007;4:637–42.
- [2] Amendola V, Meneghetti M. Nanoscale 2009;1:74–88.
- [3] Fantner GE, Oroudjev E, Schitter G, Golde LS, Thurner P, Finch MM, et al. Biophys J 2006;90:1411–8.
- [4] Guimard NK, Oehlenschlaeger KK, Zhou J, Hilf S, Schmidt FG, Barner-Kowollik C. Macromol Chem Phys 2012;213:131–43.
- [5] Hager MD, Greil P, Leyens C, van der Zwaag S, Schubert US. Adv Mater 2010;22:5424–30.
- [6] Wu DY, Meure S, Solomon D. Prog Polym Sci 2008;33:479–522.
- [7] van der Zwaag S. Bull Pol Ac Tech 2010;58:227–36.
- [8] Skrzyszewska PJ, Sprakel J, Wolf FA, Fokkink R, Stuart MAC, van de Gucht J. Macromolecules 2010;43:3542–8.
- [9] Wool RP. Soft Matter 2008;4:400–18.
- [10] Wang Q, Mynar JL, Yoshida M, Lee E, Lee M, Okuro K, et al. Nature 2010;463:339–43.
- [11] Wietor JL, Dimopoulos A, Govaert LE, van Benthem RATM, de With G, Sijbesma RP. Macromolecules 2009;42:6640–6.
- [12] White SR, Sottos NR, Geubelle PH, Moore JS, Kessler MR, Sriram SR, et al. Nature 2001;409:794–7.
- [13] Lehn J-M. PNAS 2002;99:4763–8.
- [14] Cordier P, Tournilhac F, Souli-Ziakovic C, Leibler L. Nature 2008;451:977–80.
- [15] Maes F, Montarnal D, Cantournet S, Tournilhac F, Corte L, Leibler L. Soft Matter 2012;8:1681–7.

- [16] Holten-Andersen N, Harrington MJ, Birkedal H, Lee BP, Messersmith PB, Lee KYC, et al. *PNAS* 2011;108:2651–5.
- [17] Canadell J, Goossens H, Klumperman B. *Macromolecules* 2011;44:2536–41.
- [18] Deng G, Tang C, Li F, Jiang H, Chen Y. *Macromolecules* 2010;43:1191–4.
- [19] Tuncaboylu DC, Sari M, Oppermann W, Okay O. *Macromolecules* 2011;44:4997–5005.
- [20] Tuncaboylu DC, Sahin M, Argun A, Oppermann W, Okay O. *Macromolecules* 2012;45:1991–2000.
- [21] Candau F, Selb J. *Adv Colloid Interface Sci* 1999;79:149–72.
- [22] Volpert E, Selb J, Candau F. *Polymer* 1998;39:1025–33.
- [23] Hill A, Candau F, Selb J. *Macromolecules* 1993;26:4521–32.
- [24] Regalado EJ, Selb J, Candau F. *Macromolecules* 1999;32:8580–8.
- [25] Candau F, Regalado EJ, Selb J. *Macromolecules* 1998;31:5550–2.
- [26] Kujawa P, Audibert-Hayet A, Selb J, Candau F. *J Polym Sci B Polym Phys* 2004;42:1640–55.
- [27] Kujawa P, Audibert-Hayet A, Selb J, Candau F. *Macromolecules* 2006;39:384–92.
- [28] Chern CS, Chen TJ. *Colloids Surf A Physicochem Eng Aspects* 1998;138:65–74.
- [29] Leyrer RJ, Machtle W. *Macromol Chem Phys* 2000;201:1235–43.
- [30] Miyazaki T, Kaneko T, Gong JP, Osada Y. *Macromolecules* 2001;34:6024–8.
- [31] ISO 7875-1, 1996. Water quality. Determination of surfactants. Part 1: determination of anionic surfactants by measurement of the methylene blue index (MBAS). ISO/TC 147.
- [32] Annable T, Buscall R, Ettelaie R, Whittlestone D. *J Rheol* 1993;37:695–726.
- [33] Abdurrahmanoglu S, Can V, Okay O. *Polymer* 2009;50:5449–55.
- [34] Hao J, Weiss RA. *Macromolecules* 2011;44:9390–8.
- [35] Miquelard-Garnier G, Hourdet D, Creton C. *Polymer* 2009;50:481–90.
- [36] Lin WC, Fan W, Marcellan A, Hourdet D, Creton C. *Macromolecules* 2010;43:2554–63.
- [37] Webber RE, Creton C, Brown HR, Gong JP. *Macromolecules* 2007;40:2919–27.
- [38] Lake GJ, Thomas AG. *Proc R Soc London A* 1967;300:108–19.
- [39] Livshin S, Silverstein MS. *Macromolecules* 2007;40:6349–54.
- [40] Brown HR. *Macromolecules* 2007;40:3815–8.
- [41] Sun JY, Zhao X, Illeperuma WRK, Chaudhuri O, Oh KH, Mooney DJ, et al. *Nature* 2012;489:133–6.
- [42] Fantner GE, Hassenkam T, Kindt JH, Weaver JC, Birkedal H, Pechenik L, et al. *Nat Mater* 2005;4:612–6.
- [43] Marrucci G, Bhargava S, Cooper SL. *Macromolecules* 1993;26:6483–8.
- [44] Patruyo LG, Muller AJ, Saez AE. *Polymer* 2002;43:6481–93.
- [45] Penott-Chang EK, Gouveia L, Fernandez IJ, Muller AJ, Diaz-Barríos AD, Saez AE. *Colloids Surf A Physicochem Eng Aspects* 2007;295:99–106.